Journal of Sound and Vibration (1999) **227**(2), 343–360
Article No. jsvi.1999.2349, available online at http://www.idealibrary.com on IDEAL®

THE INFLUENCE OF FAST EXCITATION ON A CONTINUOUS SYSTEM

D. TCHERNIAK

Department of Solid Mechanics, Technical University of Denmark, Building 404, *DK*-2800 *Lyngby, Denmark*

(*Received* 25 *September* 1998, *and in final form* 23 *April* 1999)

Excitation at frequency far beyond dominant resonance frequencies may affect the usual "slow" dynamics of a mechanical system. Here an examination of the effects of high-frequency excitation on a simple continuous mechanical system, a simply supported beam is presented and the possibility of utilizing high-frequency excitation to change the system's dynamical properties is considered.

1. INTRODUCTION

Excitation at frequency far beyond dominant resonance frequencies may affect the statics and dynamics of mechanical systems. This study deals with the analysis of such effects on a continuous system. The linear behaviour of a beam subjected to high-frequency excitation is considered. The possibility of controlling the dynamical properties of the beam by means of high-frequency excitation is also considered.

When a structure is subjected to "fast" excitation at a frequency which many times exceeds the lowest natural frequencies of the structure, one intuitively expects the structure to oscillate at the excitation frequency. However, when the frequency is sufficiently high, non-trivial effects may occur that cause the structure to behave quite differently. For example, equilibria may move, disappear, gain or lose stability: e.g., a pendulum subjected to fast excitation can be stable in the upward position [1] and unstable in the downward [2], and natural frequencies may change: e.g., a pendulum clock mounted on a vibrating wall can be incorrect [1]. For some other phenomena caused by fast vibration, see reference [3].

The Method of Direct Partition of Motion (MDPM) has been worked out by I.I. Blekhman as a general mathematical tool for dealing with fast excitation [4]. Based on the idea of the separation of motion into slow and fast components, the method allows one to determine the so-called "vibrational force" that accounts for the average effect of fast excitation. The MDPM has been used for a wide range of practical applications, for example the transport of granular materials or solid bodies on vibrating feeders, the separation of mixtures according to the size or density of their components, the submergence of piles, etc.

0022-460X/99/420343 + 18 $30.00/0

Thomsen has shown that the Method of Multiple Scales (MMS) can also deal with this kind of problem [5]. Similar to the MDPM, the modified MMS is based on the separation of a motion into its fast and slow components.

Using these methods, Jensen [6, 7] analyzed changes in the stability properties of two-degree-of-freedom structures subjected to fast excitation. Tcherniak and Thomsen [8] and Tcherniak [9] examined a simple one-degree-of-freedom system and showed that its linear and non-linear properties can be effectively controlled by applied fast kinematic excitation. Thomsen [10] used the MDPM to determine vibrational drift velocity.

One can consider a simple example of a continuous system: a beam. It is well-known that axial (parametric) excitation may cause dynamic instability of the straight beam configuration [11]. In contrast, *fast* axial excitation may increase beam stability: Chelomei mentioned the rise in the axial stability of a compressed rod, caused by fast longitudinal excitation, and compared this effect with the gain in stability of the upward position of a pendulum [13]. Some experimental confirmations can be found in references [3, 14]. Jensen [15] also showed that the addition of fast excitation would increase the critical axial force of the similar structure.

In contrast to the above-mentioned studies, a different approach is used here: the method of separation of motion is applied *before* system discretization. This makes it possible to obtain and analyze the partial differential equation for the slow component of motion, which will facilitate a general understanding of the effects caused by fast excitation.

The practical realization of high-frequency excitation is thought to be feasible. For example fast excitation may have a kinematic nature, e.g., could possibly be generated by ultrasonically driven piezoelectric ceramics with attached mass, which are distributed throughout the structure length. A fast oscillating excitation force changes the dynamical properties of the system, such as the natural frequencies and modes. As a result, by regulating the applied voltage, one may manipulate the slow dynamical properties of the system to adapt them to specific conditions of operation.

The paper is organized as follows: in section 2 the system to be examined is presented and its equation of motion is established; in section 3 the method of multiple scales will be applied to obtain the equations for fast and slow motion; in section 4 the slow component of motion is analyzed, the results are compared with the results of numerical simulation and the effects of shear and rotational inertia on the solution are discussed.

2. MODEL SYSTEM AND EQUATION OF MOTION

Figure 1(a) shows the system: a simply supported uniform beam subjected to time-harmonic excitation with frequency Ω^*, distributed axial load $Q(X, \Omega^* t)$ and horizontal force $P(\Omega^* t)$. Beam properties are defined by the following parameters: Young's modulus E; shear modulus G; moment of inertia I; area of the beam cross-section A; beam material density ρ. The forces acting on an elementary

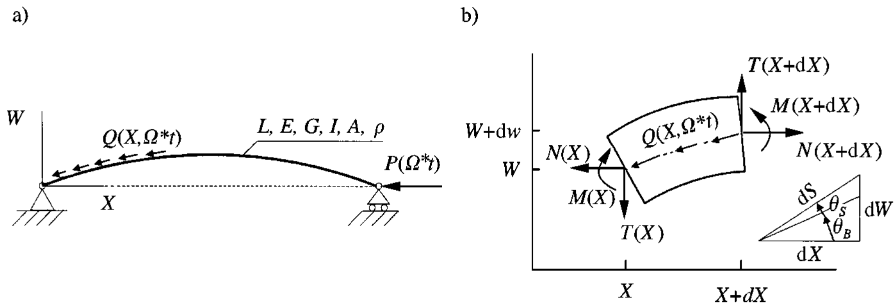

Figure 1. (a) Model system; (b) differential beam element.

segment of the beam bounded by the co-ordinate X and $X + \mathrm{d}X$ are shown in Figure 1(b).

Due to the high-frequency excitation, shear stress and rotational inertia terms have to be included in the equation of motion; thus the Timoshenko beam model will be used [16,17]. Following the standard scheme, one considers the dynamic equilibrium of the beam segment (longitudinal inertia has been disregarded):

$$M' + T - NW' = \rho I\sqrt{1 + (W')^2}\,\ddot{\theta}_B,$$

$$N = -P - \int_X^L Q(\Xi)\,\mathrm{d}\Xi,\ T' = \rho A\sqrt{1 + (W')^2}\,\ddot{W} + W'Q. \tag{1}$$

Here $(\ )' = \partial()/\partial X$, $(\dot{\ }) = \partial()/\partial t$ and $\Xi = X$ is an integration variable. The total slope is presented as the sum $\theta = \theta_B + \theta_S$, where θ_B is the slope due to bending, $\theta_B' = M/EI$, and θ_S is the slope due to shear, $\theta_s = T/kGA$, where k is known as the Timoshenko shear constant. In order to obtain the linear equation for slow motion, one has to retain non-linear terms of the second order in the equation for the total motion [9]. The resulting equation of motion is

$$\rho A\ddot{W} + EIW'''' + \frac{Ar^2\rho^2}{Gk}\ddddot{W} - \left(\frac{EI\rho}{Gk} + Ar^2\rho\right)\ddot{W}''$$

$$= \left(\frac{Er^2}{Gk}Q'' - \frac{r^2\rho}{Gk}\ddot{Q}\right)W' - \left(P + \int_X^L Q(\Xi)\,\mathrm{d}\Xi - 2\frac{Er^2}{Gk}Q'\right)W''$$

$$+ \frac{Er^2}{Gk}QW''' - 2\frac{r^2\rho}{Gk}\dot{Q}\dot{W}' - \frac{r^2\rho}{Gk}Q\ddot{W}', \tag{2}$$

where cubic and higher order non-linearities have been omitted (there are no quadratic non-linearities); $r = \sqrt{(I/A)}$ is the radius of gyration of the beam cross-section. Inertial and restoring forces are on the left and excitation terms are on the right-hand side of the equation.

Equation (2) has to satisfy the boundary conditions

$$W(0) = W(L) = 0 \text{ and } W''(0) = W''(L) = 0. \tag{3}$$

To complete the equation, dissipative terms have to be added. It is assumed that the beam material is viscoelastic and of the Kelvin–Voigt type, and the damping associated with the surrounding air is ignored. Further, the dissipation is assumed to be small so that it may be presented as a single additional term in the equation [18], $E^*I\dot{W}''''$, where E^* is the linear viscoelastic coefficient.

The equation of motion is put in a non-dimensional form by using the following set of variables:

$$x \equiv \frac{X}{L}, \quad \xi \equiv \frac{\Xi}{L}, \quad w \equiv \frac{W}{L}, \quad \omega_0 \equiv \left(\frac{\pi}{L}\right)^2 \sqrt{\frac{EI}{\rho A}}, \quad \tau \equiv \omega_0 t,$$

$$\Omega \equiv \frac{\Omega^*}{\omega_0}, \quad q(x, \Omega\tau) \equiv \frac{Q(X, \Omega^* t)}{\rho A L \omega_0^2}, \quad p(\Omega\tau) \equiv \frac{P(\Omega^* t)}{\rho A L^2 \omega_0^2},$$

$$\alpha \equiv \frac{E}{G}\frac{1}{k}\left(\frac{r}{L}\right)^2, \quad \beta \equiv \left(\frac{r}{L}\right)^2, \quad \eta \equiv \frac{E^* r}{L^2\sqrt{E\rho}}. \tag{4}$$

Here the first natural frequency of the simply supported beam ω_0 is chosen as the characteristic frequency of the system. The functions q and p describe the load oscillating at the high-frequency Ω; η denotes the internal damping; the parameters α and β reflect the effect of shear and rotational inertia, respectively (if the shear stiffness of the beam is significant, α becomes a small quantity, and, if rotational inertia can be disregarded, β should be put to zero).

The resulting non-dimensional equation becomes

$$\ddot{w} + \frac{1}{\pi^4} w'''' + \frac{\eta}{\pi^2} \dot{w}'''' + \pi^4 \alpha\beta \ddot{\ddot{w}} - (\alpha + \beta)\ddot{w}''$$

$$= \alpha(q'' - \pi^4 \beta \ddot{q}) w' - \left(p + \int_x^1 q(\xi)\,\mathrm{d}\xi - 2\alpha q'\right) w'' + \alpha q w''' - \pi^4 \alpha\beta(2\dot{q}\dot{w}' + q\ddot{w}'). \tag{5}$$

where $(\,) = \partial(\,)/\partial x$ and $(\dot{}) = \partial(\,)/\partial\tau$ now. In turn, the boundary conditions become

$$w(0, t) = w(1, t) = 0 \quad \text{and} \quad w''(0, t) = w''(1, t) = 0. \tag{6}$$

3. DETERMINING SLOW RESPONSE TO HIGH-FREQUENCY EXCITATION

Equation (5) is a non-autonomous partial differential equation. The right-hand side (the so-called *fast force*) contains a fast oscillating load and depends explicitly on time, whereas the left-hand side contains the forces that do not explicitly depend on time (inertial and *slow forces*). It is possible to suppose that the solution to equation (5) will also include correlated fast and slow components. The method of multiple scales (MMS) has been used to obtain an approximate solution. Basically, the method consists of three stages: (1) fast and slow time scales are introduced and motion is split into fast and slow components; (2) the magnitude order of the terms is determined and the problem is subdivided into several levels; (3) the solution to each level is sought to obtain the equations for slow and fast motion.

For a more detailed description of the application of MMS to non-resonant problems, see reference [5].

3.1. TIME SCALES AND SEPARATION OF MOTION

First, one can introduce a small parameter $\varepsilon = \Omega^{-1} \ll 1$. The two time scales can then be introduced as follows:

$$T_0 = \Omega\tau = \varepsilon^{-1}\tau \quad \text{and} \quad T_1 = \tau. \tag{7}$$

Here the slow time T_1 and fast time T_0 are considered to be the new independent variables of equation (5). This causes the time derivatives to be transformed according to

$$\frac{\partial^k}{\partial\tau^k} = (\varepsilon^{-1}D_0 + D_1)^k, \quad D_i^j \equiv \frac{\partial^j}{\partial T_i^j}. \tag{8}$$

Now, one can seek an approximate solution to equation (5) having the form

$$w(x, T_0, T_1) = z(x, T_1) + \varepsilon\varphi(x, T_0, T_1) + \varepsilon^2\varphi_2(x, T_0, T_1) + \mathrm{O}(\varepsilon^3), \tag{9}$$

which is required to be uniformly valid to the order ε^2. The first term of the expansion represents the slow component of w, whereas the φ-terms represent small overlays of fast motion.

3.2. MAGNITUDE ORDERING

Now, one has to set the order for two groups of coefficients in equation (5): the order of loading p and q, and the order of coefficients due to shear and rotational inertia α and β.

In the present study, the fast excitation is supposed to be large. For example, it could have a kinematic nature, (that is, some distributed mass is forced to move harmonically at high frequency but small amplitude). Thus, the excitation forces have an inertial nature and their magnitudes are proportional to the values of the moving mass, displacement and squared frequency. Using the parameter ε one can quantify them as follows:

$$q(x, \Omega\tau) = \varepsilon^{-1} q_a(x) \cos \Omega\tau, \quad p(\Omega\tau) = \varepsilon^{-1} p_a \cos \Omega\tau. \tag{10}$$

Here q_a and p_a are of the order of unity.

The orders of α and β are mainly defined by the chosen ratio r/L of the beam. After subdivision of equation (5) into orders of ε one will be concerned with the orders of ε^{-1} and ε^0. It is easy to show that α and β will appear at these order levels if they are of the order of ε^1. If

$$\alpha = \mathrm{O}(\varepsilon^2) \quad \text{and} \quad \beta = \mathrm{O}(\varepsilon^2), \tag{11}$$

the effects of shear and rotational inertia can be ignored. The expressions in equations (11) may be suggested as the criteria determining whether or not one should take the above-mentioned effects into consideration.

One can now consider case (11) and postpone examining the influence of shear and rotational inertia to section 4.6.

3.3 THE EQUATION FOR SLOW MOTION, SHEAR AND ROTATIONAL INERTIA DISREGARDED

Inserting expressions (8)–(11) into equations (5) and (6) and equating the coefficients of like powers of ε, to zero one obtains to order ε^{-1}

$$D_0^2 \varphi = f_1(z'', T_0), \tag{12}$$

where

$$f_1(z'', T_0) = -z'' n_a \cos T_0 \tag{13}$$

and

$$n_a(x) = p_a + \int_x^1 q_a(\xi)\, \mathrm{d}\xi \tag{14}$$

is a non-dimensional magnitude of the axial force $N(x, T_0)$.

To order ε^0, one has

$$D_0^2 \varphi_2 = -D_1^2 z - 2D_0 D_1 \varphi - \frac{1}{\pi^4} z'''' - \frac{\eta}{\pi^2}(D_1 z'''' + D_0 \varphi'''')$$

$$+ f_2(x, \varphi'', T_0) \equiv R(x, T_0, T_1), \tag{15}$$

where

$$f_2(x, \varphi'', T_0) = -\varphi'' n_a \cos T_0, \tag{16}$$

and boundary conditions are

$$z(0, T_1) = z(1, T_1) = 0 \quad \text{and} \quad z''(0, T_1) = z''(1, T_1) = 0. \tag{17}$$

The full solution to equation (12) is

$$\varphi(x_0, T_0, T_1) = \iint f_1(z'', T_0)\,\mathrm{d}T_0\,\mathrm{d}T_0 + T_0 c_1(x, T_1) + c_2(x, T_1), \tag{18}$$

where c_1 and c_2 are arbitrary functions. To keep φ bounded as $T_2 \to \infty$ one must let $c_1 = 0$. Also one can let $c_2 = 0$ because this function contributes nothing to the expansion (9) that cannot be accounted for by $z(x, T_1)$. Thus, the fast motions are given by

$$\varphi(x, T_0, T_1) = z'' n_a \cos T_0, \tag{19}$$

where $z = z(x, T_1)$, so that the integration is carried out by treating z as a constant in the fast time T_0. Note that the axial force and the fast motion are in *anti-phase*: that is, the beam curvature increases during the tension part of the loading period and decreases during the compression part. Such fast behaviour is typical for cases when the fast force magnitude is significant, the so-called "pure inertial approximation" [4].

Now, φ is a known function of z and T_0, one can turn to the ε^0-problem (15) for φ_2, which should be bounded to set up an equation for the determination of z (φ_2 itself is not needed). All terms of the right-hand side R are either 2π-periodic in T_0 or independent of T_0. Hence R can be expressed in exact form as

$$R(x, T_0, T_1) = \langle R(x, T_0, T_1)\rangle + H(x, T_0, T_1), \tag{20}$$

where H denotes T_0-harmonic terms and where $\langle\ \rangle$ defines the T_0-averaging operator

$$\langle R(x, T_0, T_1)\rangle \equiv (2\pi)^{-1} \int_0^{2\pi} R(x, T_0, T_1)\,\mathrm{d}T_0 \tag{21}$$

Inserting expression (20) into equation (15) one obtains

$$D_0^2 \varphi_2 = \langle R(x, T_0, T_1)\rangle + H(x, T_0, T_1). \tag{22}$$

Upon noting that $\langle R(x, T_0, T_1)\rangle$ is independent of T_0, this equation can readily be solved to yield

$$\varphi_2(x, T_0, T_1) = \tfrac{1}{2} T_0^2 \langle R(x, T_0, T_1)\rangle + \iint H(x, T_0, T_1)\,\mathrm{d}T_0\,\mathrm{d}T_0 + T_0 c_3(x, T_1) + c_4(x, T_1). \tag{23}$$

Let $c_3 = c_4 = 0$ be the same arguments that led to $c_1 = c_2 = 0$ in expression (18). The integral term remains bounded as $T_0 \to \infty$, since H is a bounded periodic function, whereas the first term in equation (23) becomes unbounded. Thus, for φ_2 to be bounded for all $T_0 > 0$, one must require $\langle R(T_0, T_1)\rangle = 0$. With φ given by expression (19), and f_1 by a function periodic in T_0 (see expression (13)) with zero mean, $\langle f_1 \rangle = 0$, one has $\langle \varphi \rangle = 0$, $\langle D_0\varphi \rangle = 0$ and $\langle D_0\varphi'''' \rangle = 0$. As a result the equation for slow motion z becomes

$$D_1^2 z + \frac{\eta}{\pi^2} D_1 z'''' + \frac{1}{\pi^4} z'''' = \langle f_2(x, \varphi'', T_0)\rangle. \tag{24}$$

Substitution into this of the known function φ, averaging and linearization into this gives

$$D_1^2 z + \frac{\eta}{\pi^2} D_1 z'''' + \frac{1}{\pi^4} z'''' = -\tfrac{1}{2} n_a n_a'' z'' - n_a n_a' z''' - \tfrac{1}{2} n_a^2 z''''. \tag{25}$$

The partial differential equation (25) with boundary conditions (17) governing the slow component $z(x, T_1)$ of $w(x, T_1, T_0)$ is the one of primary concerns. One can note that

(a) it is autonomous in T_0, since all explicit dependence on T_0 is averaged out;
(b) the left-hand side of the equation coincides with the left-hand side of the initial equation (5) (if one puts $\alpha = \beta = 0$ there) and the right-hand side is the slow term, the so-called *vibrational force* [4], accounting for the averaged effect of the fast forces;
(c) equation (25) coincides by its structure with the equation for the beam with variable stiffness $EI(x)$ but uniform mass distribution ρA: $\rho A\ddot{w} + \eta^*\dot{w}'''' + (EI(x)w'')'' = 0 \Rightarrow \rho A\ddot{w} + \eta^*\dot{w}'''' + (EI''w'' + 2EI'w''' + EIw'''') = 0$ and hence, well-known methods of analysis may be applied;
(d) the coefficients of z'', z''', z'''' depend on the function $n_a(x)$, and thus by choosing $n_a(x)$ one may change the solution to equation (25).

4. ANALYSIS OF SLOW MOTION

4.1. GALERKIN DISCRETIZATION

The partial differential equation (25) is discretized in the space co-ordinate x by Galerkin's technique, with the simply supported beam's eigenfunctions, $\sin(k\pi x)$, $k = 1, 2, 3 \ldots$ being used as a suitable set of base functions satisfying the boundary conditions (17), and $u_k(t)$ being the correspondent generalized co-ordinate; thus

$$z(x, t) = \sum_{k=1}^{K} u_k(t) \sin(k\pi x). \tag{26}$$

Considering infinitely small harmonic oscillations about the straight beam position one puts $u_k(t) = a_k e^{\lambda t}$. Inserting expression (26) into equation (25), multiplying by the shape functions $\sin(k\pi x)$ and integrating from 0 to 1, lead to the matrix equation

$$e^{\lambda t}(\mathbf{M}\lambda^2 + \mathbf{C}\lambda + \mathbf{S})\mathbf{d} = \mathbf{0}. \tag{27}$$

where $\mathbf{M} = \mathbf{I}$, $\mathbf{C}$, $\mathbf{S}$ are the mass, damping and stiffness matrixes, respectively, $\mathbf{d} = \{a_1, a_2, \dots\}^{\mathrm{T}}$ is the displacement vector. $\mathbf{C}$ is the diagonal matrix with $c_{jj} = \pi^2\eta j^4$ and thus it is positive definite. Elements of $\mathbf{S}$ depend on $n_a(x)$:

$$s_{ij} = j^4\delta_{ij} - \pi^2 j^2 \int_0^1 n_a n_a'' \sin(\mathrm{i}\pi x)\sin(j\pi x)\,\mathrm{d}x - 2\pi^3 j^3 \int_0^1 n_a n_a' \sin(\mathrm{i}\pi x)\cos(j\pi x)\,\mathrm{d}x$$

$$+ \pi^4 j^4 \int_0^1 n_a^2 \sin(\mathrm{i}\pi x)\sin(j\pi x)\,\mathrm{d}x, \tag{28}$$

where δ_{ij} is the Kronecker delta.

To simply the analysis consideration will be given only to functions such as $n_a(x)$ which are symmetric about the beam middle $x = 0{\cdot}5$. Hence the load distribution function $q_a(x)$ should be chosen antisymmetric. $q_a(x)$ is defined as

$$q_a(x) = \sum_{j=1}^{M} a_{c(2j-1)} \cos((2\mathrm{j} - 1)\,\pi x) + a_{s2j} \sin(2j\pi x), \tag{29}$$

with a_{cj}, a_{sj} denoting the Fourier coefficients. Note here that the stiffness matrix $\mathbf{S}$ is non symmetric: $s_{jk} = (jlk)^2 s_{kj}$; this means that a distributed axial (i.e., following) load preserves its non-potential nature even after averaging.

The non-trivial solution to equation (27) is K pairs $(\lambda_j, \mathbf{d}_j)$ of corresponding eigenvalues and eigenvectors. As $\lambda_j = \alpha_j + \mathrm{i}\omega_j$, where $\mathrm{i} = \sqrt{-1}$, and for α_j being non-positive, the ω_j are damped natural frequencies of the harmonic beam vibration (for any positive α_j the straight beam configuration becomes unstable). Unfortunately, it seems impossible to prove analytically that α_j are always non-positive. However, in the following numerical computations it was checked that α was non-positive. One can now start to investigate how the fast excitation value and its distribution affect the behaviour of damped natural frequencies ω_j.

4.2. A SIMPLE EXAMPLE

To demonstrate a possible influence of the fast excitation one can consider the most simple case of excitation: the beam is subjected to the horizontal force $P(\Omega t)$ only. Putting $q_a = 0$ in (25) and reintroducing D_1^2 and T_1 one obtains

$$\ddot{z} + \frac{\eta}{\pi^2}\dot{z}'''' + \left(\frac{1}{\pi^4} + \tfrac{1}{2}p_a^2\right)z'''' = 0, \tag{30}$$

which shows that the apparent stiffness of the rapidly excited beam is greater than the stiffness of the unexcited one. The stiffness matrix **S** becomes diagonal with $s_{jj} = (1 + \frac{1}{2}\pi^4 p_a^2) j^4$ and this reflects that the horizontal point-force P is potential. This system can be classified as a complete and pure dissipative system [19] and, since the matrix **S** is positive definite, the straight beam configuration is always stable ($\alpha_j \leqslant 0$).

The natural frequencies of the slow motion for the case of undamped oscillations

$$\omega_j = j^2 \sqrt{1 + \frac{\pi^4}{2} p_a^2} \tag{31}$$

are shown in Figure 2 against the axial force magnitude p_a. The spectrum of natural frequencies for the rapidly excited beam shifts towards higher frequencies, depending upon the intensity of the fast excitation applied. From small p_a the changes in the natural frequencies are very small ($\mathrm{d}\omega_j/\mathrm{d}p_a|_{pa=0} = 0$); for larger values of p_a the rise is nearly linear.

Using equation (30) one can show that the quasi-static axial stability is also increasing: the non-dimensional critical axial force for equation (30),

$$p_{crit} = \frac{1}{\pi^2} + \frac{\pi^2}{2} p_a^2, \tag{32}$$

exceeds the non-dimensional Euler force $p_{Euler} = 1/\pi^2$. This agrees with the results obtained in reference [15].

Note that to get a notable stabilization effect one has to apply a fast oscillating force whose magnitude many times exceeds the Euler force: the fast force

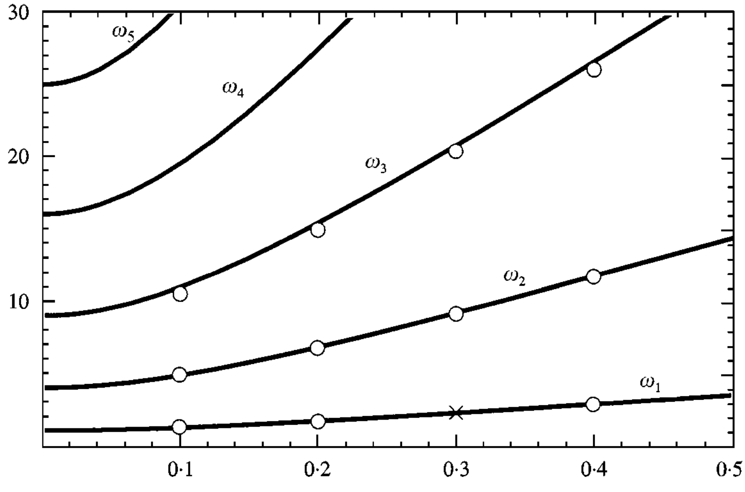

Figure 2. The first five natural undamped frequencies versus fast force magnitude. ×, The result of the numerical simulation described in section 4.3; ○, the results of the numerical simulation, parameters $\Omega = 500$, $\eta = 0{\cdot}006$.

magnitude (*cf.* expression (10)) is Ωp_a, $\Omega \gg 1$. For example, to get $p_{crit} = 1{\cdot}1\ p_{Euler}$ one should apply a fast force with magnitude approximately equal to $0{\cdot}45\ \Omega p_{Euler}$. Due to inertia the beam has no time to buckle during the compressive part of the loading period and, on average, the fast axial excitation brings about a stabilizing effect.

4.3. COMPARISON WITH NUMERICAL SOLUTIONS

To obtain a numerical solution equation (5) is rewritten as

$$\ddot{w} + \frac{1}{\pi^4} w'''' + \frac{\eta}{\pi^2} \dot{w}'''' = -\, w'' n_a \Omega \cos \Omega\tau, \tag{33}$$

where the influence of shear and rotational inertia has been disregarded by putting $\alpha = \beta = 0$, and expressions (10) and (14) were used. The boundary conditions are defined by expressions (6).

In the present study, the method of finite differences is used to reduce a partial differential equation to a system of ordinary differential equations [20]. To solve the system obtained, Adam's method was used. The main problem is that the time scales of the slow and the fast motion (for PDE (33)) are quite different; this requires many output points and hence many function evaluations. Therefore, the Shampine and Gordon 12-order variable step-size solver [21] has been used, which is useful for such cases.

Equation (33) is the equation of motion for a parametrically excited beam. The value of the excitation frequency Ω is far above the lowest natural frequencies; thus, the familiar low-mode parametric resonances cannot be provoked. However, equation (33) has a spectrum of distinct natural frequencies, thus a *number* of parametrically unstable regions appear. Nayfeh and Mook [11, pp. 319–320] mentioned that along with the conventional primary and secondary resonances, the so-called *combination* resonances occur which, unlike the first ones, can be destabilized by viscous damping. This means that resonance at high frequencies may emerge despite the viscous damping. However, in reality, these high-mode resonances are effectively suppressed by internal damping. The analysis of this high-frequency instability is beyond the scope of the present study (see reference [12] for a more comprehensive numerical analysis). When solving equation (33) we have always chosen (by trial-and-error process) the value of η to prevent any kind of this high-frequency instability for a given excitation magnitude.

For a specific set of parameters and for the specified co-ordinate $x = 0{\cdot}5$ we attempt to verify the following.

(a) Whether the slow motion, obtained as a numerical solution for equation (25), correctly captures the slow component of the full motion (obtained as a numerical solution to equation (33)) and whether the period of free small-magnitude vibration about the straight configuration corresponds to the natural frequency, obtained via Galerkin's technique.
(b) Whether two-term expansion (9) is a good approximation of the fully motion.

The results of the comparison appear in Figure 3. The beam being subjected to the fast axial force P has been initially bent to the sine-half-wave shape; and after release it starts to perform damped "quasi-free" oscillations at the frequency approximately equal to the first damped natural frequency.

In Figure 3(a) the line denoted by w shows the full motion (numerical solution to equation (33)), whereas the line denoted by z show the slow motion (numerical solution to equation (25)). One can see that the obtained slow behaviour is in good agreement with the slow component of full motion. More careful comparison with the application of a low-pass filter also confirms a good agreement between z and filtered w.

To compare the full motion and the two-term approximation (9) $z + \Omega^{-1}\varphi$ we calculate φ using expression (19). Figure 3 (b) shows $(\Omega^{-1}\varphi)$ and $(w - z)$ instead of w and $(z + \Omega^{-1}\varphi)$ because these lines, if plotted, would be indistinguishable. There is a less convincing agreement between these lines as line w lies slightly behind z as it appears from the enlarged inset in Figure 3(a). This disagreement does not affect the slow motion because the magnitudes (envelopes) of the fast components $(\Omega^{-1}\varphi)$ and $(w - z)$, shown in Figure 3(c), almost coincide (note that the vertical scale in Figures 3(b) and (c) is approximately ten times smaller than in Figure 3 (a)).

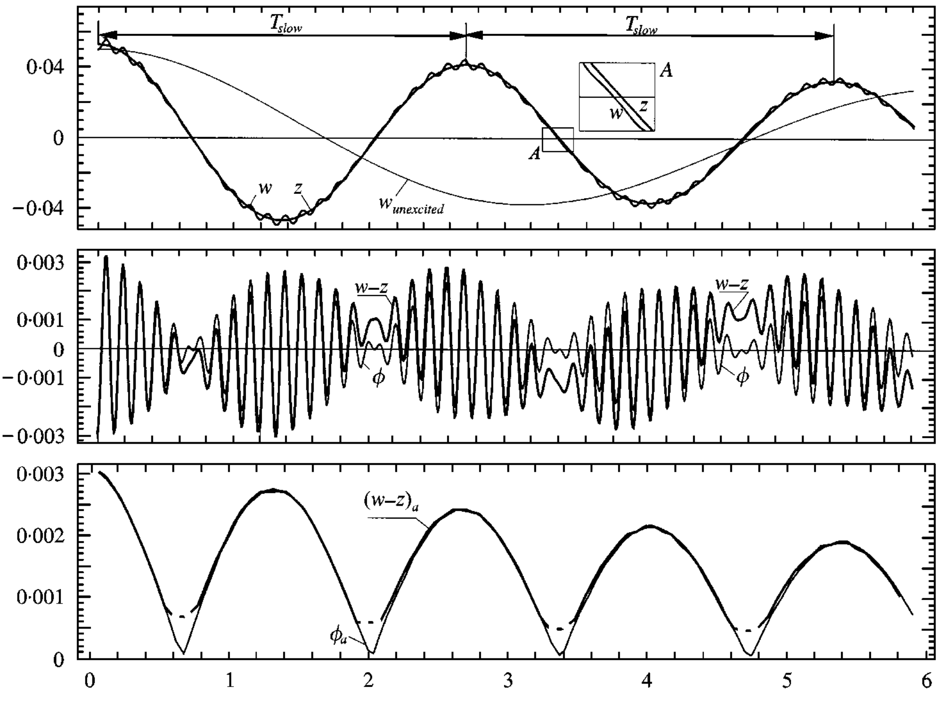

Figure 3. Numerical solution for the full motion and its two-term approximation. Top, full and slow motion; line w: numerical solution for equation (33); line z, numerical solution for equation (25); line $w_{unexcited}$, oscillations of the unexcited beam. Middle: fast motion: line φ, result of equation (19); line w–z, result of subtraction at the every time point. Bottom, fast motion envelope. Loading parameters: $p_a = 0{\cdot}3$, $q_a = 0$, $\Omega = 50$, $\eta = 0{\cdot}02$.

The period of slow oscillations T_{slow} was measured to calculate the approximate value for the first natural frequency: $T_{slow} \approx 2{\cdot}71$ and $\omega_1 = 2\pi/T_{slow} \approx 2{\cdot}32$, i.e., the applied fast excitation increases the first natural frequency more than twice: the damped oscillation of unexcited beam is shown for comparison by the thin line in Figure 3(a) ($\omega_{1\,unexcited} = 1$). This value agrees with the one obtained via Galerkin's technique (denoted by the cross in Figure 2: internal damping does not significantly affect the lowest frequencies). The performed numerical simulations (their results are denoted by the circles in Figure 2) also correspond well with the second and the third natural frequencies (for the small value of η).

Based on the results of the comparison with the numerical simulations, one may conclude that the equation for slow motion (25) is able to predict the slow component of full motion; and thus it can be used for system motion analysis.

4.4. CONTROL OF OSCILLATION MODES AND NATURAL FREQUENCIES BY SHAPING $n_a(x)$

Consider now the case when $q_a \neq 0$ and $p_a \neq 0$. By altering p_a and the coefficients a_{cj}, a_{sj} in equation (29) one shapes the function $n_a(x)$; various forms of $n_a(x)$ differently affect distinct natural frequencies and oscillation modes.

Two specific cases of loading are considered here: $p_a = 0$ and $0{\cdot}5$ for the first and the second cases respectively; $q_a(x) = a_{s2}\sin(2\pi x)$ for both cases. Schematically, the load distribution is shown in Figure 4(a, b). Negative values of q_a correspond to anti-phase excitation.

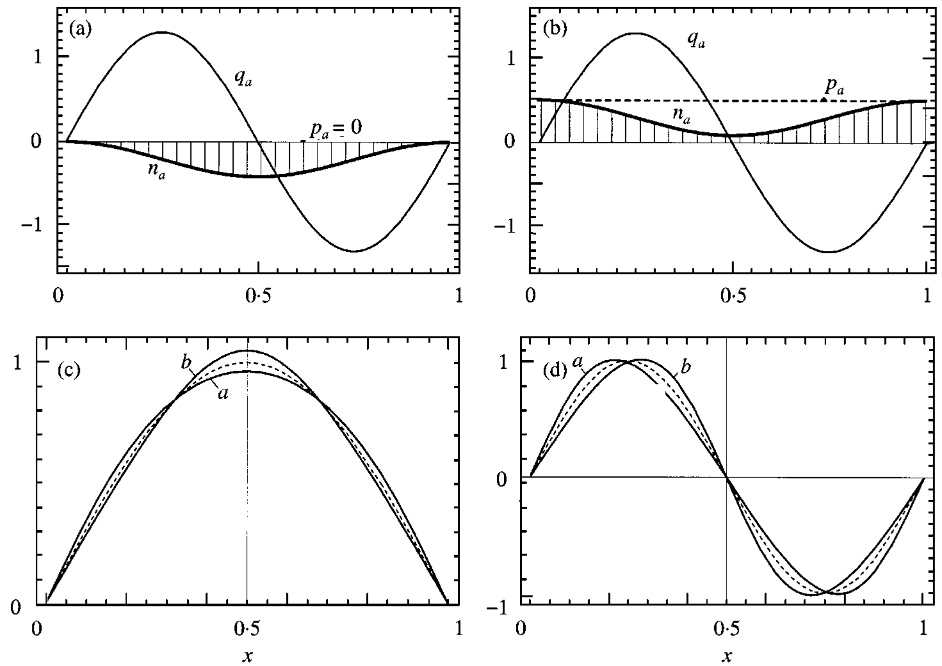

Figure 4. The loading schemes and the affected changes in the oscillation modes. Undamped oscillations. (a) $p_a = 0$, $a_{s2} = 1{\cdot}3$; (*b*) $p_a = 0{\cdot}5$, $a_{s2} = 1{\cdot}3$; (c) the 1st mode; (d) the 2nd mode. *a*, *b* denote the loading cases.

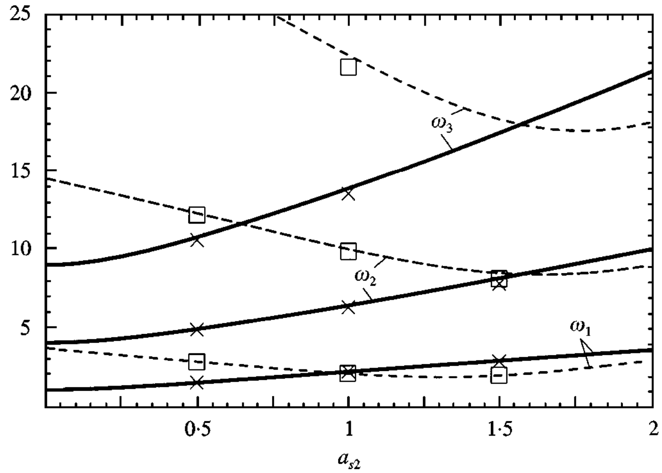

Figure 5. The first three natural frequencies versus a_{s2} for the parameters as for Figure 4. Solid line, $p_a = 0$; dashed line $p_a = 0{\cdot}5$, □, ×, numerical solutions for $\Omega = 300$, $\eta = 0{\cdot}006$.

The first and second oscillation modes are plotted in Figure 4(c, d), respectively, to compare them with the mode of the unexcited beam (dotted line). The modes of the rapidly excited beam redistribute their curvatures in a way that reduces their value where$|n_a(x)|$ has increased. For example, the first mode for the first case of loading (Figure 4(c), line *a*) becomes less curved in the middle, where the function $|n_a(x)|$ has its maximum (Figure 4(a)). In contrast, the first mode for the second case of loading (Figure 4(c), line *b*) becomes more curved in the middle; this is affected by the decrease in $|n_a(x)|$ at the beam middle. The changes in the second oscillation mode (Figure 4(d)) can be explained in a similar way.

The first three undamped natural frequencies $\omega_{1,2,3}$ for the two previously considered cases of load distribution are shown in Figure 5. Changes in the shape of $n_a(x)$ bring about significant changes in the natural frequencies. However, in any case of loading, the values of the natural frequencies exceed the corresponding ones of an unexcited beam.

By analyzing the figures, it is possible to conclude that the influence of $n_a(x)$ is similar to the influence of the stiffness distribution $EI(x)$ of a non-uniform beam: the additional (apparent) local stiffness, created by fast forces, seems to be proportional to $|n_a(x)|$. This can be compared with the usual control of dynamical properties by the additional/removal of beam material during size optimization, e.g. reference [22].

4.5. THE INFLUENCE OF INTERNAL DAMPING

The dissipative term $(\eta/\pi^2)\,\dot{w}''''$ in equation (33) effectively damps high-mode oscillations. For each value of η it is possible to find k: $\omega_k = 0$, $\alpha_k < 0$. This means that the free oscillations with frequencies above ω_k will be completely suppressed (over-damped). The influence of the fast point-force $p(q(x) = 0)$ on the first four

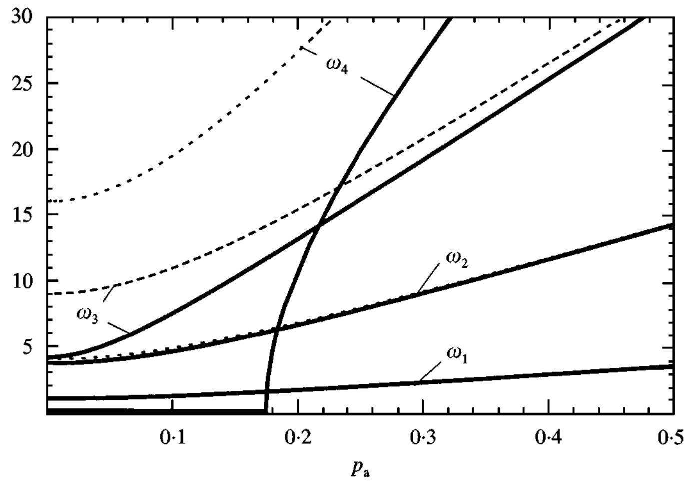

Figure 6. The first four natural frequencies for damped (solid line, $\eta = 0{\cdot}02$) and undamped (dashed line) cases.

natural frequencies is shown in Figure 6. The chosen $\eta = 0{\cdot}02$ is large enough to completely damp the oscillations at the fourth mode and significantly reduce the third damped natural frequency (note the minor damping influence on the first two modes). Applying the fast oscillating force, one may weaken the effect of the internal damping: on reaching some critical intensity of p_a, ω_4 becomes non-zero and starts to increase. Due to fast excitation, the value of ω_3 begins to increase and approaches its undamped values (dashed lines) with the fast force magnitude rising.

4.6. THE EFFECT OF SHEAR AND ROTATIONAL INERTIA

The effects of shear and rotational inertia have been disregarded in previous sections. However, if the ratio r/L of the beam is not small or excitation frequency Ω is large enough to violate criteria (11) some non-trivial effects may occur.

To define the influence of shear and rotational inertia one can consider the simple excitation model: $q = 0$ when the beam is loaded by the point-force p only.

The two time scales are introduced and the separation of motion is performed as described in section 3.1. The same load ordering as in expressions (10) is used, but now, in contrast to criteria (11),

$$\alpha = \mathrm{O}(\varepsilon) \quad \text{and} \quad \beta = \mathrm{O}(\varepsilon). \tag{34}$$

Inserting expressions (8)–(10) and criteria (34) into equation (5) and equating to zero the coefficients of like powers of ε, one obtains to order ε^{-1},

$$\pi^4 \alpha\beta\Omega^2 D_0^4 \varphi + D_0^2 \varphi = -\, z'' p_a \cos T_0. \tag{35}$$

which differs from equation (12) by the first term. Introducing $\psi = D_0^2\varphi$, dividing by $\pi^4\alpha\beta\Omega^2$ and reintroducing $D_0^k = \partial^k/\partial T_0^k$, one obtains

$$\frac{\partial^2\psi}{\partial T_0^2} + \frac{1}{\pi^4\alpha\beta\Omega^2}\psi = -\frac{z''p_a}{\pi^4\alpha\beta\Omega^2}\cos T_0. \tag{36}$$

This equation governs the forced oscillations of ψ at a frequency equal to 1. To add dissipation to the equation one may present the shear modulus (which is contained in α *cf.* expression (4)) as a complex quantity [23], $G = G_0(1 + i\delta_G)$. The introduction of the real non-dimensional $\gamma = E/G_0\ 1/k\ (r/L)^2$ yields

$$\frac{\partial^2\psi}{\partial T_0^2} + \frac{1 + i\delta_G}{\pi^4\beta\gamma\Omega^2}\psi = -(1 + i\delta_G)\frac{z''p_a}{\pi^4\beta\gamma\Omega^2}\cos T_0. \tag{37}$$

The solution to equation (37) is $\psi = \psi_0 e^{i(T_0 - \phi)}$ with the magnitude and phase given by

$$\psi_0 = -\frac{z''p_a}{\sqrt{(1 - \pi^4\beta\gamma\Omega^2)^2 + \delta_G^2}} \quad \text{and} \quad \tan\phi = \frac{\delta_G}{1 - \pi^4\beta\gamma\Omega^2}. \tag{38}$$

The resulting fast motion is the real part of $\iint\psi\, dT_0\, dT_0$:

$$\varphi = \frac{z''p_a}{\sqrt{(1 - \pi^4\beta\gamma\Omega^2)^2 + \delta_G^2}}\cos(T_0 - \phi). \tag{39}$$

The four constants of integration have been set to zero by the same arguments that led to $c_1 = c_2 = 0$ in equation (18).

Substitution of the known φ in the ε^0-problem and carrying out the same operations as have been performed in section 3.3 gives the equation for slow motion,

$$\ddot{z} + \frac{\eta}{\pi^2}\dot{z}'''' + \left(\frac{1}{\pi^4} + \tfrac{1}{2}Sp_a^2\right)z'''' = 0, \tag{40}$$

which differs from equation (30) by the coefficients S:

$$S = \frac{\cos\phi}{\sqrt{(1 - \pi^4\beta\gamma\Omega^2)^2 + \delta_G^2}}. \tag{41}$$

If the shear stiffness is not significant, or rotational inertia may be ignored, then $\phi \to 0$ and $S \to 1$, and one comes to equation (30). If the ratio r/L or the excitation frequency Ω increases then the expression $(1 - \pi^4\beta\gamma\Omega^2)$ approaches zero and an internal resonance occurs. A reasonable explanation of this is the "resonant interaction between the rotatory inertia forces — rotation resulting from bending motion — and the shear stiffness" [16]. The magnitude of the fast oscillations increases but the slow effects of the fast vibration disappear since $S \to 0$ due to $\phi \to \pi/2$. The further rise of r/L or Ω causes the phase $\phi \to \pi$ and hence makes S negative. This results in the inversion of the vibrational force action: for equation (40) the stabilizing effect of the fast axial excitation changes to a destabilizing effect.

5. SUMMARY AND CONCLUSIONS

The effects of fast harmonic excitation on the linear dynamics of a simple continuous system have been considered analytically and numerically.

In accordance with a method of separation of motion, the system's motion was split into two components: the first which slowly alters in time ("slow motion") and the second, the rapidly oscillating component ("fast motion"), overlying the first one. The expression for fast motion has been obtained. The slow motion is governed by a partial differential equation, which is simpler than the original equation of full motion. The action of the fast oscillating force is represented in the equation for slow motion by a "vibrational force", which accounts for the effects of fast excitation.

By using Galerkin's technique the PDE obtained was discretized to obtain natural frequencies and modes of quasi-free oscillations. It was shown that the fast axial point-force, acting on the beam end, increases the longitudinal beam stiffness and stability and increases its natural frequencies as well. A rapidly oscillating distributed load also changes the beam linear dynamics: by altering the value of axial force and the shape of the distributed load, it is possible to change natural frequencies and modes and thus control the system's linear dynamics.

Further it was shown that fast axial excitation changes the influence of internal damping: for example, the free oscillations in higher modes, completely suppressed by internal damping, may be released by high-frequency vibration.

The effects of shear and rotational inertia were looked into. To determine when one should take these effects into consideration, we have proposed a criterion, relating the beam geometry to the excitation frequency. It is shown that the above-mentioned effects can change the sign of the vibrational force; this leads to quite the opposite action of fast excitation: destabilization instead of stabilization, etc.

Despite its simplicity, the system considered has features of many engineering structures. The results of this investigation may thus contribute to the general understanding and utilization of high-frequency excitation.

Obviously, experimental studies are needed to confirm the presence of the effects considered and verify the possibility of their utilization in engineering. More detailed investigation into the effects of shear and rotational inertia seems to be necessary.

ACKNOWLEDGMENT

The author wishes to thank all members of the "Fast Vibration Club" for many invaluable suggestions and fruitful discussions.

REFERENCES

1. P. L. Kapitza 1951 *Zurnal Eksperimental'noj i Teoreticeskoj Fiziki* **21**, 588–597. Dynamic stability of a pendulum with an oscillating point of suspension (in Russian).
2. J. M. Schmitt and P. V. Bayly 1998 *Nonlinear Dynamics* **15**, 1–14. Bifurcations in the mean angle of a horizontally shaken pendulum: analysis and experiment.
3. V. N. Chelomei 1983 *Soviet Physics Doklady* **28**, 387–390. Mechanical paradoxes caused by vibrations.
4. I. I. Blekhman 1994 *Vibrational Mechanics* (in Russian). Moscow: Fizmatlit Publishing Company. (To appear in English translation by World Scientific Publishing Company, 1999).
5. J. J. Thomsen 1999 *DCAMM Report* (to appear), Technical University of Denmark. Using perturbation methods to study slow effects of fast, non-resonant excitation.
6. J. S. Jensen 1998 *Journal of Sound and Vibration* **215**, 125–142. Nonlinear dynamics of the follower-loaded double pendulum with added support-excitation.
7. J. S. Jensen 1999 *Nonlinear Dynamics* (in press). Pipes conveying fluid pulsating with high frequency.
8. D. M. Tcherniak and J. J. Thomsen 1998 *Nonlinear Dynamics* **17**, 227–246. Slow effects of fast harmonic excitation for elastic structures.
9. D. M. Tcherniak 1998 *Proceedings of the IUTAM/IFToMM Symposium on Synthesis of Nonlinear Dynamical Systems—SNDS'98*, Riga Latvia. Using fast vibration to change the non-linear properties of mechanical system.
10. J. J. Thomsen 1998 *Proceedings of the IUTAM/IFToMM Symposium on Synthesis of Nonlinear Dynamical Systems—SNDS'98*, Riga Latvia. Vibration-induced displacement using high-frequency resonators and friction layers.
11. A. H. Nayfeh and D. T. Mook 1979 *Nonlinear Oscillations*. New York: Wiley.
12. M. H. Hansen, 1999 *DCAMM Report* (No. 601) Technical University of Denmark. Non-trivial effects of high-frequency excitation of spinning disks.
13. V. N. Chelomei 1956 *Soviet Physics Doklady* **110**, 345–347. On the possibility to increase an elastic systems stability by means of vibration (in Russian).
14. S. V. Chelomei 1981 *Soviet Physics Doklady* **26**, 390–392. Dynamic stability upon high-frequency parametric excitation.
15. J. S. Jensen 1999 *International Journal of Non-linear Mechanics* (in press). Nonlinear behaviour of a buckled beam with high-frequency excitation.
16. R. W. Traill-Nash and A. R. Collar 1953 *Quarterly Journal of Mechanics and Applied Mathematics* VI, 186–222. The effect of shear flexibility and rotatory inertia on the bending vibrations of beams.
17. L. H. Donnell 1976 *Beams, Plates and Shells*. New York: McGraw-Hill.
18. M. P. Païdoussis and C. Semler 1993 *Journal of Fluids and Structures* **7**, 269–298. Nonlinear dynamics of a fluid-conveying cantilevered pipe with an intermediate spring support.
19. H. Ziegler 1968 *Principles of Structural Stability*. Walton: Blaisdell.
20. T. Iwatsubo, M. Saigo and Y. Sugiyama 1973 *Journal of Sound and Vibration* **30**, 65–77. Parametric instability of clamped–clamped and clamped-simply supported columns under periodic axial load.
21. L. F. Shampine and M. K. Gordan 1975 *Computer Solution of Ordinary Differential Equations: The Initial Value Problem* San Francisco: Freeman.
22. A. P. Seyranian, F. Solem and P. Pedersen 1998 *DCAMM Report* No. 577, Technical University of Denmark, Multi-parameter linear periodic systems: sensitivity analysis and applications.
23. J. C. Snowdon 1968 *Vibration and Shock in Damped Mechanical Systems*. New York: Wiley.